DOI: 10.1002/ejic.200800431

A Mixed-Valence [$Mn^{II}Mn^{III}Mn^{II}$] Complex of a Linear Phenol–bis(pyrazole) Ligand with an $S = 3$ Spin Ground State

Leoní A. Barrios,[a] Guillem Aromí,*[a] Joan Ribas,[a] Jorge Salinas Uber,[b] Olivier Roubeau,[c] Ken Sakai,[d] Shigeyuki Masaoka,[d] Patrick Gamez,[b] and Jan Reedijk*[b]

Keywords: Pyrazole ligands / Manganese / Antiferromagnetic coupling / Mixed-valence complexes / Ligand design

A novel ligand featuring one phenol and two pyrazole groups in a linear fashion was prepared. This donor facilitates the assembly of a mixed-valence chain of Mn ions in the [$Mn^{II}Mn^{III}Mn^{II}$] sequence, with formula [$Mn_3(Hpbpz)_2(OAc)_3(MeOH)_3$] (**1**). Complex **1** exhibits dominant antiferromagnetic coupling between adjacent pairs of Mn ions. A fit of the magnetic susceptibility data using the Hamiltonian $H = -2J_1(S_1S_2 + S_2S_3) - 2J_2(S_1S_3)$ yields coupling constants of $J_1 = -3.14\ cm^{-1}$ and $J_2 = -0.39\ cm^{-1}$, which leads to a spin ground state of $S_T = 3$.

Introduction

The rational design and preparation of coordination metal clusters is an important research area in magnetochemistry as remarkable metal–metal interactions may be obtained through the formation of such assemblies.[1,2] The generation of polynuclear complexes may be achieved by the appropriate choice of ligand(s), which should favour close contact between metal ions and therefore produce potentially interesting physical properties.[3] In that context, the use of bridging ligands is paramount to produce cluster coordination compounds.[4] Among the various bridging ligands used to create polynuclear complexes, the pyrazolate moiety has allowed the preparation of outstanding compounds.[5–7] The simple phenolate unit may also act as a bridging ligand to generate clusters with unusual magnetic properties.[8] Therefore, the inclusion of phenol and pyrazole rings within a single ligand molecule may lead to a bridging system able to assist in the self-assembly of novel polynuclear aggregates. Successful examples of such an application of mixed pyrazole/phenol ligands to synthesize cluster compounds have been recently reported.[9–12]

In the course of our investigations aimed at preparing polynuclear metal complexes with attractive magnetic properties, a series of phenol–bis(β-diketonate) ligands were created and their coordination chemistry studied.[13–15] For instance, the bridging bis(β-diketone) ligand 2-hydroxy-5-methyl-1,3-bis(3-oxo-3-phenylpropionyl)benzene (H_3ptk) was successfully used to generate metal clusters of various nuclearities.[16,17] It is well known that the pyrazole ring can be obtained by reaction of a β-diketone with hydrazine.[18] This reaction has now been exploited for the formation of a novel group of poly(pyrazole) ligands, from the available poly(β-diketone) analogues, as a new entry into original coordination clusters. Indeed, the reaction of H_3ptk with hydrazine yields the potentially pentadentate (upon deprotonation of the pyrazole N–H groups and the phenolic function) ligand 4-methyl-2,6-bis(5-phenylpyrazol-3-yl)phenol (H_3pbpz, Scheme 1, see Exp. Sect.). A close derivative of this ligand, with methyl groups instead of phenyl groups, has previously been used in coordination chemistry.[19] We report here the synthesis and structure of a mixed-valence trinuclear $Mn^{II}Mn^{III}Mn^{II}$ coordination compound prepared with H_3pbpz, together with its magnetic properties.

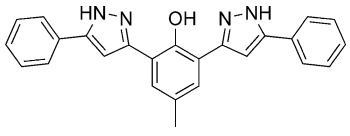

Scheme 1. H_3pbpz.

[a] Departament de Química Inorgànica, Universitat de Barcelona, Diagonal 647, 08028 Barcelona, Spain
Fax: +34-93-4907725
E-mail: guillem.aromi@qi.ub.es
[b] Leiden Institute of Chemistry, Gorlaeus Laboratories, Leiden University,
P. O. Box 9502, 2300 RA Leiden, The Netherlands
[c] Université Bordeaux 1, CNRS-CRPP,
115, avenue du Dr. Schweitzer, 33600 Pessac, France
[d] Department of Chemistry, Faculty of Science, Kyushu University,
Hakozaki 6-10-1, Higashi-ku, Fukuoka 812-8581, Japan
Supporting information for this article is available on the WWW under http://www.eurjic.org or from the author.

Results and Discussion

Synthesis and Molecular Structure

The reaction of $Mn(OAc)_2{\cdot}4H_2O$ with H_3pbpz (3:2 molar ratio) in methanol at room temperature produced upon slow concentration brown block-shaped crystals, suitable for synchrotron X-ray crystallography.

The identity of the product was established as $[Mn_3(Hpbpz)_2(OAc)_3(MeOH)_3](MeOH)$ (**1**·MeOH), and its structure is depicted in Figure 1 (and Figure S1). Selected bond lengths and angles of **1** are given in Table 1. This complex consists of a chain-like arrangement of three manganese ions held together by two doubly deprotonated $Hpbpz^{2-}$ ligands acting as tetradentate N_3O donors. The ligand bridges one outer Mn ion with the central Mn atom through a phenoxide bridge, and the latter metal atom with the third metal atom via a deprotonated pyrazolate moiety (an N–N bridge). The other pyrazole group remains neutral and participates in the chelation of one of the external metal atoms through the inner nitrogen atom. Thus, as anticipated, the phenol–bis(pyrazole) ligand promotes the formation of a metal cluster. Additional negative charges are provided by three acetate anions; one acting as a μ_3-bridge of the three metal atoms, the other two being terminal ligands of the outer metal atoms. In fact, the former acetate is disordered over two positions (which are crystallographically equivalent) with occupancy factors of 0.5 (Figure 2). Hexacoordination of the Mn ions is completed by three MeOH molecules, one on each metal atom. The latter are in the oxidation state +2 (Mn1 and Mn3) and +3 (Mn2). This assignment is consistent with the valence-bond sum analysis[20] and the magnetic behaviour of the compound (see below). This implies that part of the metal atoms experience aerial oxidation driving the formation of a stable mixed-valence compound. A few chain-type trinuclear clusters of mixed manganese ions +2/+3 exist. However, most of them are of the $[Mn^{III}–Mn^{II}–Mn^{III}]$ type,[21,22] while those with $[Mn^{II}–Mn^{III}–Mn^{II}]$,[23,24] such as complex **1** are scarcer.

Table 1. Selected bond lengths [Å] and angles [°] for $[Mn_3(Hpbpz)_2(OAc)_3(MeOH)_3]$ (**1**).

Mn1–O2	2.317(3)	Mn1–O10	2.234(4)
Mn1–O3	2.164(3)	Mn1–N1	2.302(3)
Mn1–O5	2.258(3)	Mn1–N7	2.254(3)
Mn1–O12	2.257(5)		
N1–Mn1–N7	98.33(10)	O5–Mn1–N7	85.81(10)
O5–Mn1–O10	92.50(15)	O10–Mn1–N1	80.00(15)
O5–Mn1–O12	77.35(17)	O12–Mn1–N1	96.96(17)
O2–Mn1–O3	172.05(10)		
Mn2–O1	1.974(3)	Mn2–O10	2.382(5)
Mn2–O2	1.963(3)	Mn2–N2	2.012(3)
Mn2–O6	2.286(3)	Mn2–N6	2.004(4)
Mn2–O13	2.297(5)		
O1–Mn2–O6	91.52(13)	O2–Mn2–O6	91.61(10)
O2–Mn2–O10	74.22(13)	O1–Mn2–O10	102.74(15)
O2–Mn2–O13	105.40(14)	O1–Mn2–O13	71.56(16)
N2–Mn2–N6	178.86(14)		
Mn3–O1	2.319(3)	Mn3–O11	2.365(5)
Mn3–O7	2.188(3)	Mn3–N3	2.259(4)
Mn3–O9	2.247(3)	Mn3–N5	2.309(4)
O1–Mn3–O11	93.95(14)	O7–Mn3–O11	85.64(14)
O7–Mn3–N3	104.50(11)	O1–Mn3–N3	78.80(12)
O1–Mn3–O13	67.77(16)	O7–Mn3–O13	108.77(15)
Mn1–O2–Mn2	104.71(11)	Mn1–O10–Mn2	96.64(18)
Mn2–O1–Mn3	105.54(14)	Mn2–O13–Mn3	99.8(2)
Mn1···Mn2	3.395(2)	Mn2···Mn3	3.425(2)
Mn1···Mn3	5.931(2)	Mn1–Mn2–Mn3	120.82(3)

The three metal ions are in distorted octahedral environments with N_2O_4 donor sets. The distortion is most likely due to the steric constraints imposed by the rigidity of the $Hpbpz^{2-}$ ligands and the presence of the μ_3-acetato group. Ions Mn1 and Mn3 exhibit the same coordination geometry consisting of two almost identical disordered forms with 50% occupancy (Figure 2). Both environments are formed by two N atoms from monodentate and bidentate pyrazole

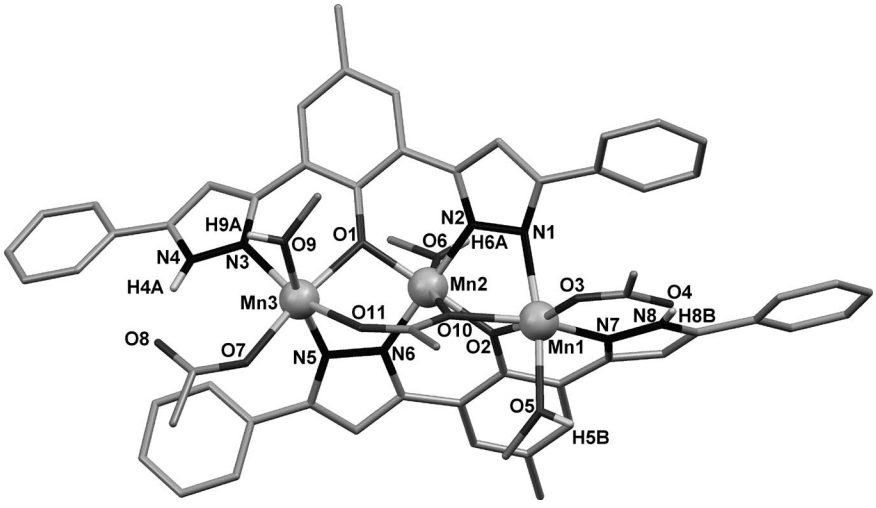

Figure 1. Representation of the crystal structure of $[Mn_3(Hpbpz)_2(OAc)_3(MeOH)_3]$ (**1**). Only the hydrogen atoms involved in hydrogen-bonding interactions are shown. The lattice methanol molecule is omitted for clarity. Only one of the disordered bridging acetate ligands is shown.

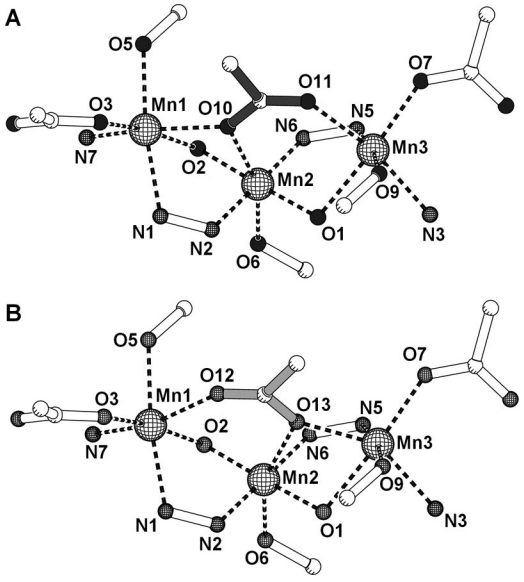

Figure 2. Illustration of the two crystallographic positions (each with an occupancy factor of 0.5) adopted by the acetate anion bridging the atoms Mn1, Mn2 and Mn3.

rings, respectively, two O atoms from a bridging phenolato and a μ_3-acetato ligand, and two O atoms from monodentate acetato and methanol ligands, respectively. The central Mn2 atom is in a Jahn–Teller elongated octahedral environment, whose basal plane is constituted of two bidentate pyrazolato N atoms and two phenolato O atoms, with axial positions occupied by a methanol molecule and an O atom from the μ_3-acetato ligand (in two equivalent disordered positions; O10 and O13, Figure 2). Within this assembly, the adjacent Mn···Mn distances are 3.395(2) Å (Mn1–Mn2) and 3.425(2) Å (Mn2–Mn3), respectively, and the Mn1–Mn3–Mn2 angle is 120.82(3)°. The Mn–N and Mn–O bond lengths for the three metal centres (Table 1) are within the ranges previously observed for this type of coordination environment.[25]

Compound **1** shows strong intramolecular hydrogen-bonding interactions between the pyrazole N–H groups and the monodentate acetate ions [N4–H4A···O8 2.785(5) Å, N4–H4A–O8 154° and N8–H8B···O4 2.773(4) Å, N8–H8B–O4 155°; see Figure 1 for atom numbering]. In addition, the acetate atoms O4 and O8 are involved in strong intermolecular hydrogen bonds with coordinated methanol molecules [$O5^{i}$ and $O9^{ii}$, respectively; symmetry codes: (i) $-x, -y + 2, -z + 1$; (ii) $-x, -y + 2, -z$] from neighbouring trinuclear units [O4···$H5B^{i}$–$O5^{i}$ 2.711(4) Å, O4–$H5B^{i}$–$O5^{i}$ 171° and O8···$H9A^{ii}$–$O9^{ii}$ 2.721(4) Å, O8–$H9A^{ii}$–$O9^{ii}$ 170°] generating a one-dimensional supramolecular chain. Finally, the lattice methanol molecule (O1S) is hydrogen-bonded to the methanol molecule (O6) coordinated to Mn2 [O6–H6A···O1S 2.741(5) Å, O6–H6A–O1S 175°].

Magnetic Properties

Bulk magnetization data were collected from a powdered microcrystalline sample of **1**, under a constant magnetic field of 3 kG in the 2–300 K temperature range. A $\chi_M T$ vs. T plot is shown in Figure 3. The product $\chi_M T$ at 300 K is 12.10 $cm^3 K mol^{-1}$ (the expected value for an uncoupled, high-spin, $Mn^{II}_2Mn^{III}$ system with $g = 2$ is 11.75 $cm^3 K mol^{-1}$) and decreases with cooling to 3.48 $cm^3 K mol^{-1}$ at 2 K, showing a small step near 12 K at 5 $cm^3 K mol^{-1}$. This behaviour clearly suggests that the coupling in **1** is dominated by antiferromagnetic interactions between the Mn^{II} ($S = 5/2$) and Mn^{III} ($S = 2$) ions leading to a total spin ground state $S_T = 3$. The decrease after the small step is attributed to zero field splitting (ZFS) of the ground state, or to antiferromagnetic interactions. The coupling within complex **1** is well described by the Heisenberg spin Hamiltonian $H = -2J_1(S_1S_2 + S_2S_3) - 2J_2(S_1S_3)$, by using the scheme shown in Figure 3, where $S_1 = S_3 = 5/2$ and $S_2 = 2$. This Hamiltonian may be transformed into $H = -J_1(S_T^2 - S_A^2 - S_2^2) - J_2(S_A^2 - S_1^2 - S_3^2)$ by using the Kambe vector coupling approach[26] and the definitions $S_A = S_1 + S_3$ and $S_T = S_A + S_2$. The solutions to this Hamiltonian are $E(S_T,S_A) = -J_1[S_T(S_T + 1) - S_A(S_A + 1)] - J_2[S_A(S_A + 1)]$, where the constant terms have been eliminated. With these solutions, an expression of $\chi_M = f(T)$ may be obtained, based on the Van Vleck equation, which was fitted to the experimental data. In this fit, the ZFS and/or intermolecular interactions where modelled by using a Curie–Weiss temperature term θ, whereas a temperature-independent paramagnetism (TIP) of 600×10^{-6} $cm^3 K mol^{-1}$ was included. A very good fit (Figure 3, solid line) resulted for the following parameters: $J_1 = -3.14$ cm^{-1}, $J_2 = -0.39$ cm^{-1}, $g = 2.10$ and $\theta = -2.1$ K. These results lead to an $S = 3$ ground state with an $S = 2$ excited state lying 8.7 cm^{-1} above in energy. The value of g is slightly higher than expected for Mn systems, although this parameter commonly experiences errors when determined through bulk magnetic data. On the other hand, it needs to be kept in mind that the parameter θ includes two effects, therefore, no precise physical meaning can be ascribed to it.[27] It should be pointed out that an $S_T = 3$ ground state may be achieved for a large collection of (J_1;J_2) values; in fact, with the model used, these two parameters are highly correlated in the curves that fit well with the data. This can be observed in the error surface of the fit of $\chi_M T$ to the

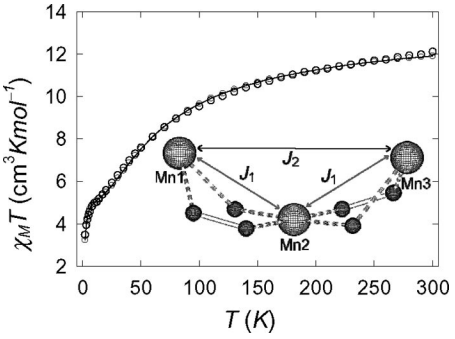

Figure 3. $\chi_M T$ vs. T plot per mol of $[Mn_3(Hpbpz)_2(OAc)_3(MeOH)_3]$ (**1**). The solid line is the best fit to the experimental data. The inset shows the spin coupling scheme.

experimental data (Figure 4) where the root-mean-square error (see Supporting Information)[28] is represented as a function of J_1 and J_2, with g and θ fixed at 2.10 and –2.1 K, respectively. In this contour, a deep "valley" of smallest error is observed, illustrating the correlation existing between both coupling constants in this region. Despite this correlation, a minimum of error occurs for the values provided by the fitting procedure, as can be observed clearly in Figure 4. In this Figure, only a limited area of the $[J_1;J_2]$ space is represented. Nevertheless, a larger area was explored that did not provide any other error minimum.

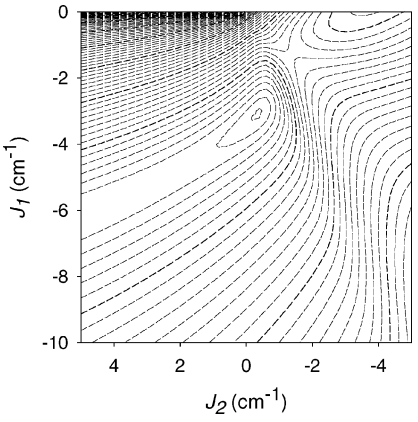

Figure 4. Contour projection (dashed lines) of the fit error of the $\chi_M T$ vs. T plot of **1**, as a function of J_1 and J_2, calculated for g and θ constant at 2.10 and –2.1 K, respectively.

In the linear mixed-valence $[Mn^{II}–Mn^{III}–Mn^{II}]$ chain complexes previously reported, the magnetic behaviour is dominated by the coupling between $Mn^{II}Mn^{III}$ pairs. Thus, when this coupling is ferromagnetic[24,29,30] the ground state is $S_T = 7$, while for the case where the interaction is antiferromagnetic,[31,32] the ground state is $S_T = 3$. Only in one exception is this coupling constant and that between the external metal atoms comparable and negative.[33] In this case, the nature of the ground state remains ambiguous, postulated to lie between $S_T = 1$ and 3.

The nature of the ground state of complex **1** was studied by means of isofield reduced magnetization measurements. Plots of $M/N\mu_B$ vs. H/T are represented in Figure 5. The curves at different fields do not superimpose, indicating the presence of a zero field splitting (ZFS).

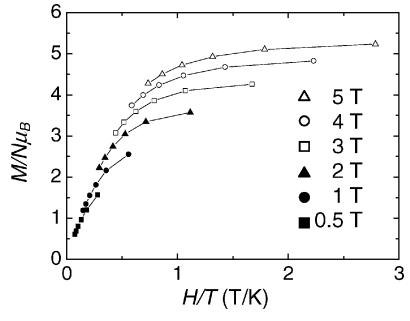

Figure 5. Variable-temperature isofield $M/N\mu_B$ vs. H/T plots for complex **1** at the indicated constant magnetic fields. The solid lines are guides to the eye.

For the largest magnetic field employed (5 T) the saturation tends to occur near 5.3 units, significantly below the expected value for $S_T = 3$ ($M/N\mu_B = 6$ if $g = 2.0$). Attempts to simulate these data were conducted through a full diagonalization numerical procedure by using the Hamiltonian $H = g\beta S_T B + D[S_{Tz}^2 - S(S + 1)/3] + E(S_{Tx}^2 - S_{Ty}^2)$, under the assumption that only the ground state is populated (D and E are the ZFS parameters and S_{Ti} are the components of the total spin operator). These did not produce any acceptable fit or set of satisfactory parameters, which was attributed to the fact that likely, under the conditions of the measurements, some excited states are partially occupied. This is consistent with the low saturation values exhibited by the reduced magnetization plots, and prevents us from using this method to estimate the magnitude of the ZFS parameters of the ground state. Nevertheless, the possibility for slow relaxation of the magnetization of complex **1** resulting from a magnetoanisotropy energy barrier exists. This behaviour was probed by means of AC susceptibility measurements at various frequencies (see Exp. Sect.), which revealed very weak frequency-dependent signals for the out-of-phase component of the susceptibility beginning to emerge below 3 K (see Figure S4). Such observation could be attributed to the manifestation of superparamagnetic-like behaviour in complex **1**; however, this has to be confirmed through investigations at lower temperature.

Conclusions

Incorporation of two pyrazole moieties separated by a phenol group into a ligand serves to promote the assembly of a chain $[Mn_3]$ cluster, following the reaction of this ligand with $Mn(OAc)_2$. The new cluster is one of the few mixed-valence triads reported with an $[Mn^{II}–Mn^{III}–Mn^{II}]$ sequence, and its topology is enforced by the structure of the multinucleating ligand. This molecule exhibits an $S_T = 3$ ground state resulting from dominant antiferromagnetic interactions between adjacent metal atoms, which appears to experience slow relaxation of its magnetization below 3 K. The potential of ligand H_3pbpz for the assembly of novel magnetic coordination clusters is now being explored.

Experimental Section

Ligand H_3pbpz: H_3ptk[34] (0.50 g, 1.25 mmol) was dissolved in MeOH (50 mL). Hydrazine monohydrate (1 mL, 1.03 g, 20.6 mmol) was added to this solution, and the reaction mixture was refluxed for 1 h. The resulting light-yellow precipitate was isolated by filtration. The solid was washed with MeOH (3 × 20 mL) and dried at 50 °C under reduced pressure for 12 h. Yield of pure H_3pbpz: 0.43 g (87%). $C_{25}H_{20}N_4O$ (392.45): calcd. C 76.51, H 5.14, N 14.28; found C 76.55, H 5.28, N 14.27. ES(+)-MS: m/z = 392.83 $[M + H]^+$. IR (neat solid): $\tilde{\nu}$ = 3416, 2858, 1616, 1558, 1471, 1366, 1274, 1238, 1171, 1074, 1022, 994, 966, 852, 800, 762, 744, 691, 636, 548, 513 cm^{-1}. ^{1}H NMR (300 MHz, [D$_6$]DMSO): δ = 2.34 (s, 3 H), 7.21 (s, 2 H) 7.25–7.55 (m, 6 H), 7.64 (s, 2 H), 7.85 (d, 4 H), 11.60 (s, 1 H), 11.87 (s, 2 H) ppm.

Complex 1: H_3pbpz (20.0 mg, 0.05 mmol) was suspended in MeOH (5 mL). Next, a solution of manganese(II) acetate tetrahydrate (18.7 mg, 0.08 mmol) in MeOH (5 mL) was added to the ligand solution. The resulting reaction mixture was refluxed for 30 min. The orange-brown solution was filtered, and the filtrate was left unperturbed for the slow evaporation of the solvent. After 24 h, brown block-shaped crystals were collected and air-dried (yield: 24.4 mg, 77%, based on Mn). Air exposure led to absorption of one molecule of water. $C_{60}H_{61}Mn_3N_8O_{12}+H_2O$ (1250.99+18.02): calcd. C 56.79, H 5.00, N 8.83; found C 57.15, H 5.12, N 9.03. IR (neat solid): $\tilde{\nu}$ = 3309, 3054, 2921, 2831, 1538, 1532, 1472, 1447, 1423, 1394, 1263, 1202, 1178, 1142, 1017, 860, 822, 758, 752, 692, 648, 556, 493, 466, 452 cm^{-1}.

X-ray Crystallographic Analysis: Crystallographic data and refinement details are given in Table 2. Intensity data were collected by using synchrotron radiation (λ = 0.8129 Å) at the Daresbury station 16.2smx. The structure was solved with direct methods and refined over F^2 with the SHELXTL package.[35] The bridging acetate moiety was disordered over two adjacent positions, and its distances were restrained to be similar. All hydrogen atoms were found in difference Fourier maps and were placed geometrically on their riding atom. Some residual electron density peaks remained, probably corresponding to partial lattice methanol molecules, which could not be modelled satisfactorily. The corresponding areas were analyzed and taken into account with PLATON/SQUEEZE[36], which recovered 78 electrons per cell in a large void of 851 $Å^3$. The combination of these two numbers would account reasonably for about four diffuse methanol molecules. CCDC-689915 contains the supplementary crystallographic data for this paper. These data can be obtained free of charge from The Cambridge Crystallographic Data Centre via www.ccdc.cam.ac.uk/data_request/cif.

Table 2. Crystallographic data for complex $[Mn_3(Hpbpz)_2(OAc)_3(MeOH)_3](MeOH)$ (**1**·MeOH).

Empirical formula	$C_{59}H_{57}Mn_3N_8O_{11}\cdot CH_4O$
Formula mass	1250.99
Space group	$P\bar{1}$
a [Å]	12.0763(11)
b [Å]	13.305(5)
c [Å]	24.398(8)
α [°]	79.281(15)
β [°]	87.803(15)
γ [°]	75.698(11)
V [$Å^3$]	3732.3(19)
Z	2
Temperature [K]	150(2)
λ [Å]	0.8129
$D_{calcd.}$ [$mg\,m^{-3}$]	1.113
μ [mm^{-1}]	0.793
Final R indices [$I > 2\sigma(I)$]	R_1 = 0.0566
	wR_2 = 0.1537
Final R indices (all data)	R_1 = 0.0788
	wR_2 = 0.1658
G.O.F.	1.046

Physical Measurements: Variable-temperature magnetic susceptibility data were obtained with a Quantum Design MPMS5 SQUID magnetometer. Pascal's constants were utilized to estimate diamagnetic corrections to the molar paramagnetic susceptibility. The AC magnetic susceptibility measurements were conducted with an alternating field of 3 Oe, above 1.8 K at frequencies ranging from 123 to 1488 Hz. The powdered sample used was analyzed and revealed substitution of MeOH molecules by H_2O. Anal. calcd. (found) for **1**(–3MeOH+2.5H_2O) (1167.88): C 57.59 (57.67), H 4.32 (4.19), N 9.59 (9.50). Elemental analyses were performed in-house with a Perkin–Elmer Series II CHNS/O Analyzer 2400, at the Servei de Microanàlisi of CSIC, Barcelona, Spain, or at Leiden University with a Perkin–Elmer 2400 series. IR spectra (4000–300 cm^{-1} range) were recorded with a Bruker 330V IR spectrophotometer equipped with a Golden Gate Diamond. ^1H NMR spectra were recorded with a Bruker DPX 300 (300 MHz) instrument. Chemical shifts are reported in δ (parts per million) relative to an internal standard of tetramethylsilane. ESI mass analyses were carried out with a Voyager Elite from PerSeptive Biosystems.

Supporting Information (see footnote on the first page of this article): ORTEP representation of Complex **1**, equation used for calculation of the error of the fitting of magnetic data, fit and surface error of the susceptibility of complex **1** for θ = 0, and plots of χ_M'' vs. T from AC measurements.

Acknowledgments

We acknowledge the provision of time at the CCLRC Daresbury Laboratory through the support of the European Union.

[1] C. I. Yang, W. Wernsdorfer, Y. J. Tsai, G. Chung, T. S. Kuo, G. H. Lee, M. Shielh, H. L. Tsai, *Inorg. Chem.* **2008**, *47*, 1925–1939.
[2] C. J. Milios, R. Inglis, R. Bagai, W. Wernsdorfer, A. Collins, S. Moggach, S. Parsons, S. P. Perlepes, G. Christou, E. K. Brechin, *Chem. Commun.* **2007**, 3476–3478.
[3] P. J. Steel, *Coord. Chem. Rev.* **1990**, *106*, 227–265.
[4] G. Aromí, E. K. Brechin, *Struct. Bonding (Berlin)* **2006**, *122*, 1–67.
[5] M. Stollenz, C. Große, F. Meyer, *Chem. Commun.* **2008**, 1744–1746.
[6] A. K. Boudalis, B. Donnadieu, V. Nastopoulos, J. M. Clemente-Juan, A. Mari, Y. Sanakis, J. P. Tuchagues, S. P. Perlepes, *Angew. Chem. Int. Ed.* **2004**, *43*, 2266–2270.
[7] S. Trofimenko, *Prog. Inorg. Chem.* **1986**, *34*, 115–210.
[8] A. L. Barra, A. Caneschi, D. Gatteschi, D. P. Goldberg, R. Sessoli, *J. Solid State Chem.* **1999**, *145*, 484–487.
[9] Y. L. Bai, J. Tao, W. Wernsdorfer, O. Sato, R. B. Huang, L. S. Zheng, *J. Am. Chem. Soc.* **2006**, *128*, 16428–16429.
[10] J. Tao, Y. Z. Zhang, Y. L. Bai, O. Sato, *Inorg. Chem.* **2006**, *45*, 4877–4879.
[11] M. Viciano-Chumillas, S. Tanase, G. Aromí, J. M. M. Smits, R. de Gelder, X. Solans, E. Bouwman, J. Reedijk, *Eur. J. Inorg. Chem.* **2007**, 2635–2640.
[12] S. Tanase, G. Aromí, E. Bouwman, H. Kooijman, A. L. Spek, J. Reedijk, *Chem. Commun.* **2005**, 3147–3149.
[13] G. Aromí, P. Gamez, J. Krzystek, H. Kooijman, A. L. Spek, E. J. MacLean, S. J. Teat, H. Nowell, *Inorg. Chem.* **2007**, *46*, 2519–2529.
[14] G. Aromí, J. Ribas, P. Gamez, O. Roubeau, H. Kooijman, A. L. Spek, S. Teat, E. MacLean, H. Stoeckli-Evans, J. Reedijk, *Chem. Eur. J.* **2004**, *10*, 6476–6488.
[15] G. Aromí, C. Boldron, P. Gamez, O. Roubeau, H. Kooijman, A. L. Spek, H. Stoeckli-Evans, J. Ribas, J. Reedijk, *Dalton Trans.* **2004**, 3586–3592.
[16] G. Aromí, P. Gamez, O. Roubeau, H. Kooijman, A. L. Spek, W. L. Driessen, J. Reedijk, *Angew. Chem. Int. Ed.* **2002**, *41*, 1168–1170.
[17] G. Aromí, P. C. Berzal, P. Gamez, O. Roubeau, H. Kooijman, A. L. Spek, W. L. Driessen, J. Reedijk, *Angew. Chem. Int. Ed.* **2001**, *40*, 3444–3446.
[18] F. Gosselin, P. D. O'Shea, R. A. Webster, R. A. Reamer, R. D. Tillyer, E. J. J. Grabowski, *Synlett* **2006**, 3267–3270.
[19] S. K. Dutta, K. K. Nanda, U. Florke, M. Bhadbhade, K. Nag, *J. Chem. Soc., Dalton Trans.* **1996**, 2371–2379.
[20] W. T. Liu, H. H. Thorp, *Inorg. Chem.* **1993**, *32*, 4102–4105.

[21] N. Kitajima, M. Osawa, S. Imai, K. Fujisawa, Y. Morooka, K. Heerwegh, C. A. Reed, P. D. W. Boyd, *Inorg. Chem.* **1994**, *33*, 4613–4614.
[22] V. Tangoulis, D. A. Malamatari, G. A. Spyroulias, C. P. Raptopoulou, A. Terzis, D. P. Kessissoglou, *Inorg. Chem.* **2000**, *39*, 2621–2630.
[23] X. S. Tan, J. Sun, C. H. Hu, D. G. Fu, D. F. Xiang, P. J. Zheng, W. X. Tang, *Inorg. Chim. Acta* **1997**, *257*, 203–210.
[24] A. Yoshino, T. Miyagi, E. Asato, M. Mikuriya, Y. Sakata, K. Sugiura, K. Iwasaki, S. Hino, D. Hino, *Chem. Commun.* **2000**, 1475–1476.
[25] K. Shindo, Y. Mori, K. Motoda, H. Sakiyama, N. Matsumoto, H. Okawa, *Inorg. Chem.* **1992**, *31*, 4987–4990.
[26] A. Cornia, D. Gatteschi, K. Hegetschweiler, *Inorg. Chem.* **1994**, *33*, 1559–1561.
[27] Note that for the mean-field approximation to be valid, θ must be one order of magnitude smaller than the other intramolecular interactions. Here θ is larger than J_2; however, in this case it accounts for both, the intermolecular interactions as well as the effects of zero field splitting, which for $S = 3$ involving Mn^{III}, must not be negligible. The use of θ to model the low-temperature part of the curve helps to improve the quality of the fitting, and does not disrupt the appropriate estimation of J_1, J_2 and g. In fact, a good fit of the curve excluding θ was obtained for the experimental data down to 12 K, which yielded similar values of these parameters, and the corresponding error surface shows the same kind of correlation between J_1 and J_2 as that obtained including θ (see Figures S2 and S3 in the Supporting Information).
[28] G. Aromí, S. Bhaduri, P. Artus, J. C. Huffman, D. N. Hendrickson, G. Christou, *Polyhedron* **2002**, *21*, 1779–1786.
[29] V. Pavlishchuk, F. Birkelbach, T. Weyhermuller, K. Wieghardt, P. Chaudhuri, *Inorg. Chem.* **2002**, *41*, 4405–4416.
[30] R. T. W. Scott, S. Parsons, M. Murugesu, W. Wernsdorfer, G. Christou, E. K. Brechin, *Chem. Commun.* **2005**, 2083–2085.
[31] J. C. Liu, Y. Xu, C. Y. Duan, S. L. Wang, F. L. Liao, J. Z. Zhuang, X. Z. You, *Inorg. Chim. Acta* **1999**, *295*, 229–233.
[32] T. Tanase, S. Tamakoshi, M. Doi, M. Mikuriya, H. Sakurai, S. Yano, *Inorg. Chem.* **2000**, *39*, 692–704.
[33] D. J. Price, S. R. Batten, K. J. Berry, B. Moubaraki, K. S. Murray, *Polyhedron* **2003**, *22*, 165–176.
[34] G. Aromí, P. Gamez, P. C. Berzal, W. L. Driessen, J. Reedijk, *Synth. Commun.* **2003**, *33*, 11–18.
[35] G. M. Sheldrick, *SHELXTL*, Bruker AXS, Madison, **1997**.
[36] P. Vandersluis, A. L. Spek, *Acta Crystallogr., Sect. A* **1990**, *46*, 194–201.

Received: April 27, 2008
Published Online: July 11, 2008

